

OPTICAL ABSORPTION AND ELECTRICAL CONDUCTIVITY
IN CASSITERITE

By

JOHN WILLARD NORTHRIP II

W

Bachelor of Science

Southwest Missouri State College

Springfield, Missouri

1954

Submitted to the faculty of the Graduate School of
the Oklahoma State University of Agriculture and
Applied Science in partial fulfillment of the
requirements for the degree of
MASTER OF SCIENCE
May, 1958

NOV 7 1958

OPTICAL ABSORPTION AND ELECTRICAL CONDUCTIVITY
IN CASSITERITE

Thesis Approved:



Thesis Adviser



Dean of the Graduate School

410281

ACKNOWLEDGMENT

I wish to express the greatest appreciation to all who have helped on this project. It is with the deepest gratitude that I thank Dr. E. E. Kohnke not only for his help in setting up and working on the project, but for the many long conversations in which he guided me past the pitfalls which beset the novice in research. Special thanks also goes to Dr. W. J. Leivo for the discussions we have had on the fundamental principles underlying the study of the solid state. I wish to thank Dr. H. E. Harrington and other members of the Physics Department staff for their encouragement and assistance throughout my graduate study.

Special recognition and thanks are given to Thomas Young, Curtis Johnson, and John Wayland, my co-workers in the solid state laboratory, for the advice, questions, answers, and discussions they have given while we were working together. On the technical side, I wish to thank R. C. Robertson of the Physics Department shop for his help in the preparation of samples and equipment. I would also like to thank the Special Services Department of the Oklahoma State University Library for help in obtaining reprints of various articles.

And in closing, I wish to express my deepest thanks to my wife, Charlotte, who has given me encouragement and understanding throughout the work.

TABLE OF CONTENTS

Chapter	Page
I. INTRODUCTION	1
II. REVIEW OF LITERATURE	5
III. DESCRIPTION OF SAMPLES AND EXPERIMENTAL EQUIPMENT.	14
A. Description of Samples.	14
B. Preparation of Samples.	16
C. Optical Equipment	16
D. Conductivity Equipment.	22
IV. OPTICAL DATA AND CALCULATIONS.	27
V. ELECTRICAL MEASUREMENTS AND CALCULATIONS	35
A. Preliminary Measurements.	35
B. Conductivity vs. Temperature Data	37
VI. CONCLUSIONS AND SUGGESTIONS FOR FURTHER STUDY.	45
A. Correlation of Optical and Thermal Activation Energies.	45
B. Suggestions for Further Work.	47
BIBLIOGRAPHY.	50

LIST OF TABLES

Table	Page
I. Tabulated Optical Data and Corresponding Activation Energies	34
II. Calculated Activation Energies and Temperature Ranges in Which They Were Found	44
III. Correlated Activation Energies	46

LIST OF FIGURES

Figure	Page
1. Mount for Beckman Spectrophotometer.	20
2. Mount for Perkin-Elmer Spectrometer.	20
3. High Temperature Conductivity Mount.	20
3a. Cutaway View	20
4. Circuit Schematic for Room Temperature Resistivity Measurements	21
5. Circuit Schematic for Conductivity vs. Temperature Measurements	21
6. Transmission Spectrum of Sample I.	31
7. Transmission Spectrum of Sample II	31
8. Transmission Spectrum of Sample III.	32
9. Transmission Spectrum of Sample SI	32
10. Transmission Spectrum of Sample AI	33
11. Conductivity vs. Temperature Curve for Sample I.	40
12. Conductivity vs. Temperature Curve Showing Degree of Homogeneity in Sample II	41
13. Conductivity vs. Temperature Curve for Sample II	42
14. Conductivity vs. Temperature Curve for Sample SI	43

CHAPTER I

INTRODUCTION

Although oxides have been used for many years as ceramics and refractories, interest in their properties as semiconductors is of more recent origin. As such they constitute a very interesting group because they lie in that region between the pure ionic materials and the materials which are primarily electronic in their electrical character. Thus work on oxides can be correlated with that on other important semiconductors including many sulfides, tellurides, selenides, and certain halides. Oxides may be studied in forms ranging from loose powders through sintered materials to thin films and large single crystals. In general their melting points are high and they are fairly stable at low temperatures. However, a wide variation of properties may be found among samples of the same oxide, primarily dependent upon method of preparation and thermal history.

While certain oxides (copper oxide, zinc oxide, magnetic iron oxide) have been studied rather extensively, information on this group as a whole is scattered and no single conduction model has come forward to explain all of the experimental results. In recent years study has also been started on the leading member of a particular family of oxides, rutile (1, 2, 3). It is the purpose of this study to extend the investigations to a second member of the rutile group, cassiterite.

Cassiterite is the crystalline form of stannic oxide, and as such is the principal ore of tin. It characteristically occurs in high temperature igneous veins, usually being found with granite or quartz. It is also a common alluvial material in regions containing granitic formations. Commercially its principal use is in the production of tin. The mineral was mined as early as the fifteenth century in several European countries. During the eighteenth and nineteenth centuries England supplied most of the mineral from the mines near Cornwall. At present there are important known deposits in Indonesia, Australia, Japan, South Africa, and Bolivia. Although this mineral is found in many places scattered throughout the United States, no extensive deposits have been discovered (4).

Crystals of cassiterite vary in color from colorless to yellow, reddish brown, and opaque brownish black. As a rule the color is distributed through the crystal in bands, and much of the transparent crystal material occurs in such bands included between portions of opaque material. These crystals have a hardness between six and seven, and a specific gravity near seven. Chemically the material is insoluble in water, acids, and organic solvents, but it can be dissolved in alkalis with the formations of gels or sols of stannic hydroxide (5).

Cassiterite is a birefringent material with both indices of refraction near two. It sometimes exhibits dichroism with the absorption of the extraordinary ray greater than that of the ordinary. The indices of refraction increase with increases of temperature but the

birefringence tends to decrease. Birefringence increases with increasing wavelength (4). Crystallographically, cassiterite is a member of the rutile group of tetragonal crystals, of the form known as ditetragonal dipyramidal. It normally exists with a large amount of twinning, giving highly irregular crystals. Cleavage tends to be indistinct with the best parting on the 111 or 011 planes (4).

Tin oxide having the cassiterite structure has found many uses in addition to its value as an ore. One of the first materials to be introduced deliberately for producing opacity in glasses, glazes, and enamels, it is used extensively as a base for colored glazes, especially red and yellow ones (6). In recent years it has found uses in high temperature refractories since it shows great resistance to thermal shock and corrosion by oxidizing atmospheres (7). In conjunction with rutile powders it has been used in development of a ceramic body having a very low temperature coefficient of capacitance (6). Powdered cassiterite has also found some use in industrial chemistry as a catalyst in the oxidation of hydrocarbons, the hydrogenation of benzene compounds, and the manufacture of hydrogen and carbon monoxide from hydrocarbons (8). Thin films showing the cassiterite structure are being used as a transparent, electrically conducting layer on glass in de-icing equipment (9).

Patents have been issued for other uses involving special electrical and optical properties of cassiterite. Treatment with a small amount of titanium ions gives green luminescence upon irradiation with ultraviolet light or electron beams (10). Pressure dependent electrical resistance granules, suitable for use in a microphone, are prepared by treating cassiterite granules with

hydrogen (11). Industrial electrical contacts may be made of silver containing two to fourteen percent powdered tin oxide (12).

Although the purpose of the project of which this study is the first phase is basic research, a better understanding of the fundamental properties of stannic oxide will conceivably lead to new developments in its use.

CHAPTER II

REVIEW OF THE LITERATURE

Too much has been written on the general properties of semi-conducting oxides for a comprehensive survey of that field to be given here, but three useful and representative review articles on the subject are those of Verwey (13) and Gray (14, 15). Verwey discusses the conductivity of oxidic semiconductors from the viewpoint of stoichiometry, dilution, and controlled valency. He also considers the effects of impurities and boundary layers between crystals. Gray, on the other hand, is primarily concerned with the effect of the surrounding atmosphere on the surface and near surface portions of the material. He gives a discussion of the adsorption and desorption of oxygen under various conditions.

Since certain properties of cassiterite might be expected to be similar to those of rutile, because of the corresponding crystal structure, a survey of the principal work on the optical and electrical properties of rutile single crystals has been made. Although semiconductor studies on rutile have only been undertaken in the past few years, quite a body of information has been built up showing important characteristics of this material. One of the first of these is its extremely high dielectric constant. Studies on sintered samples give an average dielectric constant near 110 (16). Connell and Seale (17) studied the dielectric constant in the frequency range 0-50 Kc. and reported an anomalous dispersion in this range. However Berberich and

Bell (18) reported that the dielectric constant was essentially constant in the radio frequency range (ca 114), falling off rapidly in the infra-red region to a value of 7.42. They also report a similar situation with cassiterite, the dielectric constant being 24 at low frequencies and falling to 4.11 in the optical region.

The most extensive investigations of the electrical and optical properties of single rutile crystals have been those of Cronmeyer (1, 2) and of Breckenridge and Hosler (3). Using both single crystal and ceramic samples, Cronmeyer took measurements of optical absorption, photoconductivity, Hall effect, and conductivity vs. temperature and correlated them with calculated activation energies based on a simple atomic model. He reports an intrinsic energy gap of 3.05 ev and an activation energy of 0.74 ev. On the other hand, Breckenridge and Hosler used conductivity vs. temperature and Hall measurements to determine mobility and charge carrier concentrations. These were then correlated with a model in which activation energies were calculated assuming trivalent titanium ion sites and oxygen vacancies. Mobilities were described in terms of interaction of carriers with the non-isotropic lattice. Breckenridge and Hosler predict an intrinsic gap of 3.67 ev, based on Cronmeyer's previous measurements and activation energies as low as 0.01 ev. Cronmeyer's 3.05 ev activation energy is assigned by them to the excitation of an electron from a neutral or singly-ionized Ti^{+3} - oxygen vacancy center to the conduction band.

Other studies on the semiconducting properties of rutile have centered on the effects of different impurities on the electrical and

optical properties. Johnson (19) has made an extensive study of the effect of small additions of oxides containing anions of several different valencies on the conductivity of rutile. He found that impurities having a valence greater than four had a marked effect on the conductivity and attributed this to the production within the crystal of large numbers of trivalent titanium ions. Also, together with Weyl (20), he has studied the effects of trivalent titanium ions and oxygen vacancies on the electrical properties and color of single crystals. They attribute most of the color changes to the presence of oxygen vacancies. Zerfoss, Stokes, and Moore (21) found that oxidation of opaque crystals produced a change to transparent bluish crystals and then to yellow ones. Weyl and Forland (22) made investigations into the effect of light on adsorption and desorption of oxygen at the surface of rutile and the consequent change of optical properties. All of these investigations disclose different ways in which the properties of rutile crystals can be markedly changed.

Other results worthy of note include the observation of electroluminescence in single rutile crystals by Harmon and Raybold (23). From the long infrared absorption spectrum of rutile, Matossi (24) has detected the presence of "quasimolecules" of TiO within the crystal structure. These are due to greater than normal bonding energies between certain oxygen and titanium ions. Based on the crystal structure of the material, Mitchell (25) has predicted that there should be two separate impurity activation energies from the fact that an impurity atom can replace either a central or a corner titanium ion in the unit cell.

During the last half of the nineteenth century, artificial crystals identified as having cassiterite composition and structure were discovered in the firebrick lining of certain tin smelters. Arzruni (26) reported on the finding of several such crystals in a smelter near Salzburg. These crystals had evidently grown over a period of years in corrosion pockets in the furnace lining. He speculated that they might have been formed either by vapor condensation or by precipitation from a saturated solution but was unable to give any special support to either contention. Two of these crystals have been obtained and plans to compare some of their properties with those of natural crystals have been made.

At about the same time Levy and Bourgeois (27) produced microscopic platelets and needles by precipitation from tannic acid solution. They reported that stannic oxide crystals having a different structure from the ordinary cassiterite were formed. Wunder (28) also reported this polymorphism existing in microscopic crystals grown in flame using a borax bead flux. However, modern writers list only one crystal structure for stannic oxide, the cassiterite (rutile) structure (29). Recent attempts to grow artificial cassiterite crystals suitable for semiconducting studies have proved unsuccessful (30).

In the early part of the present century much work was done on the crystal structure of the rutile group and on the special structure of cassiterite itself. A review of the findings is given by Vegard (31). In this he lists the various crystal parameters and lattice spacings as determined from x-ray diffraction patterns. Bollnow (32) has calculated the bonding energies to be expected for both the rutile and

the cassiterite structures. Using x-ray diffraction, Bragg and Darbyshire (33) investigated the crystal structure of very thin films of oxidized tin and discovered that they exhibited the same structure as natural cassiterite.

Because no method has been found for successfully growing macroscopic single cassiterite crystals, investigations of the electrical and optical properties have had to deal with either natural crystals, sintered samples, or thin films of the material. The inhomogeneity of natural crystals makes investigation of their electrical properties difficult, while sintered samples are of little use in optical measurements. The finding by Bragg (33) that the cassiterite structure is retained in very thin films of stannic oxide has opened a field of study that permits both electrical and optical investigations, but thin films themselves give rise to other experimental difficulties.

Neuhaus and Noll (34) investigated variations in properties among samples of natural cassiterite, variations which they attributed to impurity content of the samples. Himmel (35) made optical investigation on crystals from several sources, studying primarily their indices of refraction and birefringence. Although the indices of refraction of all his samples were very nearly the same, he reported variations in the change of birefringence with changes of incident wavelength. Gotman (36) reported other anomalies in the angle between the optic axes from a study of fourteen samples of natural cassiterite from the U. S. S. R.

Ecklebe (37) made a comprehensive study of the temperature variation of optical properties of a crystal from Bolivia. He studied the index of refraction and the optical absorption for visible light (400 to 720 millimicrons) in the temperature range 16-1100^o C. Using polarized light, he obtained results for both the ordinary and extraordinary ray in all of his measurements. He reported a short wavelength cutoff at 430 millimicrons for 400^o C which moved to 620 millimicrons as the temperature rose to 1100^o C. By the use of a photographic plate for detection of ultraviolet light, he found that this absorption moved to 375 millimicrons at room temperature. Berton (38) gave a value of 332 millimicrons for a similar cutoff at room temperature.

Liebisch (39) tested several crystals of cassiterite while searching for crystal detectors. He found that these crystals seemed to be sensitive on the natural pyramidal surfaces. His article contains a spectroscopic study of several crystals of cassiterite showing the presence of aluminum, calcium, iron, titanium, and tungsten as major impurities with many other elements appearing in specific samples.

Tonneson (40) recently included cassiterite crystals among some 300 solids in a study of the distribution of transistor action. Using a bar cut from a crystal as a filamentary transistor he was able to get a gain of 3.3 over the emitter signal. This compared with gains of 3.4 for silicon and 1.5 for germanium under the same conditions. However, he states that the results obtained would probably vary greatly with surface treatment, a factor not considered in his study.

As stated before, most of the work on sintered samples of stannic oxide has been in the study of its electrical conductivity. LeBlanc and Sachse (41) gave a value of this conductivity at room temperature as 10^{-8} reciprocal ohm-centimeters. Guillery (42) measured conductivity at low temperatures, using samples in the form of powder dielectrics (the method of Volkl) as well as sintered tablets. He obtained values varying from 10^{-8} to 10^{-4} reciprocal ohm-centimeters.

The most comprehensive study made of the electrical conductivity of stannic oxide powders is that of Foex (43). His samples consisted of finely pulverized oxide compressed into small cylinders at a pressure of 3,000 kilograms per square centimeter. Measurements of the resistance were made as a function of the temperature in the range 20-1200° C and as a function of the atmosphere. His resistance vs. temperature curves show straight line portions both at high temperatures and near room temperature. If it is assumed that in these areas the conductivity varies according to the equation,

$$\sigma = \sigma_0 e^{-\frac{\Delta E}{kt}}$$

The activation energies, ΔE , are calculated as 1.77 ev from the high temperature slope and 0.38 ev from the other. He reported the highest resistance for samples heated and cooled in an oxygen atmosphere. These samples tended to have a slightly greater resistivity after cooling than before heating. Samples heated in a nitrogen atmosphere had resistances while being heated which were near those of samples in oxygen, but had much smaller resistances on the cooling cycle. Samples heated in air gave essentially the same results as those heated in oxygen, while samples heated in vacuum reacted about the

same as those heated in nitrogen. He also reported a difference in resistivity depending on the method of preparation of the stannic oxide.

One optical study that has been made on powders is that of Luckeish (44). He studied the ultraviolet reflection from many common substances, among them stannic oxide used as a white pigment and reported that the reflectance of this pigment falls off sharply in the region from 3600 Angstroms to 3200 Angstroms. This corresponds with the absorption region reported earlier for crystals of cassiterite.

Bauer (45) formed thin films of stannic oxide on quartz by first evaporating metallic tin onto the quartz to a thickness of 0.1 to 10 microns and then heating this in oxygen to 800° C. Low temperature conductivity measurements on these films gave results indicating activation energies on the order of 0.02 ev near 100° K, and 0.05 ev near room temperature. A Hall measurement showed that the Hall constant was always negative with an absolute value near $0.35 \text{ cm}^3/\text{amp sec}$. The electron mobility was calculated to be 0.9 to $6.6 \text{ cm}^2/\text{volt sec}$.

Lyon and Geballe (46) made measurements on tin oxide coated glass at low temperatures. They used samples of commercially coated conducting glass in the temperature range 1- 300° K. In this range the resistance of the samples varied as an exponential power of temperature. They also reported that after going to very low temperatures they sometimes had to wait as long as twenty hours for the resistance to reach an equilibrium value.

Fischer (47) made measurements on films showing the cassiterite structure and having a thickness on the order of 700 millimicrons. He found conductivities to be about 30 reciprocal ohm centimeters and Hall

constants near $-0.2 \text{ cm}^3/\text{amp sec}$. Calculations indicated a free electron concentration of the order of 10^{20} per cubic centimeter, and a mobility of $6 \text{ cm}^2/\text{volt sec}$. He also calculated the intrinsic energy gap to be 4.1 ev, somewhat higher than the value given by other authors..

Aitcheson (48) investigated the effect of impurities on the conduction of films ranging in thickness from 100 to 400 millimicrons. He found that the introduction of trivalent ions in the form of indium tended to increase the resistivity, while the introduction of pentavalent ions such as antimony caused a decrease. This he explained on the assumption that the majority of carriers were furnished by oxygen vacancies which reduced the Sn^{+4} ions to Sn^{+3} with addition of antimony tending to enhance this action and addition of indium tending to offset it.

Andrievskii and Zhuravlev (49) investigated photoconductivity in thin films of cassiterite, and found very long relaxation times for this effect. Upon illumination of the films the photocurrent would continue to rise for periods as long as two hours and when the light source was removed a period of sixteen to twenty hours was required for it to fall to an equilibrium value. The rate of fall could be expressed as a sum of exponentials, suggesting that the long time constant might be due to a series of trapping centers within the crystalline lattice.

CHAPTER III

DESCRIPTION OF SAMPLES AND EXPERIMENTAL EQUIPMENT

A. Description of Samples

In this study the experimental work was done on five different cassiterite crystals chosen in such a way as to provide a wide variation in properties and appearance at room temperature.

Three of the samples were taken from the same crystal. This crystal was for the most part opaque and had a rust brown color. However, it did exhibit a definite layer structure and one of the layers was quite transparent. One of the samples was taken from the opaque material and was cut in a rectangular parallelepiped (Sample I). Two more samples were cut from the clear layer. The first of these was in the form of a bar (Sample II), while the other was in the shape of a slab (Sample III). Sample III was very transparent showing few flaws except in one corner where a brown coloration was observed. Sample II, on the other hand, had a definite discontinuity about two-thirds of the way down its length, being quite transparent in the longer portion and brown (although still slightly transparent) in the shorter. Several inclusions and one large fault plane were visible in the region near the barrier. Studies with a polarizing microscope indicate that both Samples II and III were cut with their broadest faces perpendicular to the optic axis.

Two small crystals from Araca, Bolivia, were obtained through the courtesy of the Smithsonian Institute (Smithsonian Inst. Cat.

No. R-8034). These crystals also were primarily opaque but had a definite bluish color and each had a transparent layer on one surface. One of the layers was cut off to form a slab (Sample SI). Thus one face of the sample was a natural pyramidal surface while the other was a cut surface. Although quite transparent, this sample was darker than Samples II and III, and had a slightly smoky appearance.

Near the end of the study reported here, two samples of artificial cassiterite crystals found many years ago in the tin smelters near Salzburg were obtained through the kindness of Professor M. Weil of the University of Strasbourg, France. These crystals were transparent and of a violet color but contained a large number of inclusions. One of the crystals was used for optical measurements (Sample AI), but electrical measurements have not yet been attempted.

The dimensions of the five samples were as follows:

<u>Sample</u>	<u>Length</u> (mm)	<u>Width</u> (mm)	<u>Thickness</u> (mm)	<u>Appearance</u>
I	5.6	3.9	1.4	Opaque reddish brown
II	6.2	2.2	1.5	Clear over most of length but containing a definite discontinuity
III	5.7	3.2	0.95	Very clear
SI	7.4	5.3	1.0	Transparent but smoky
SI (after cutting down for resistance measurements)				
	2.7	1.3	1.0	Same as before
AI	Irregular			Violet with large inclusions

B. Preparation of Samples

In preparing Samples II and III for optical measurements, two opposite faces were polished using jewelers' rouge and fine alundum powder. Some difficulty was encountered in getting an optical finish on the cut surfaces. Several times large portions of the surface would tend to "tear" off just as it was approaching a smooth finish, probably due to the layer structure of the crystal. The cut side of Sample SI was treated the same way, but the natural face was left untouched. All of the samples were stored in compartments in a small wooden sample box, with each sample wrapped in lens tissue. It was not felt necessary to keep them under dessication since they are apparently unaffected by atmospheric moisture.

Several methods of cleaning were used. After general use, the samples were cleaned by soaking them in an acetone bath and were also swabbed gently with filter paper which had been soaked in acetone. This was followed by a rinse in methyl alcohol since the acetone sometimes tended to leave a film on the polished surfaces. After certain of the high temperature measurements, a metallic film was found on portions of the sample. This was removed by soaking the sample in nitric acid for about five minutes, after which the acid was rinsed off with liberal quantities of distilled water. This procedure removed all signs of contamination without visibly affecting the crystal.

C. Optical Equipment

The optical measurements in the ultraviolet, the visible, and the near infrared regions of the spectrum were taken by means of the

Beckman DK-1 Spectrophotometer. This is a double beam ratio recording instrument utilizing quartz optics to obtain an operating range from 185 millimicrons to 3500 millimicrons. The circuitry is such that linear recording is possible for wavelength vs. percent transmittance, absorbance, or energy, with several different ranges available.

For near infrared and visible measurements (3500 to 350 millimicrons) a tungsten source is used and the radiation is detected by means of a lead sulfide detector. The high dispersion of the quartz prism in this range allows near monochromatic beams to be selected.

In the ultra violet region (350 to 185 millimicrons) a hydrogen lamp is used as the source and a sensitive photomultiplier tube is used as detector. The photomultiplier tube has a sensitivity range from 185 to 600 millimicrons which permits its use in the overlapping portions of the ranges.

Light from the source entering the monochromator is chopped at a frequency of 480 cycles per second, the optimum operating frequency for the lead sulfide cell. Upon leaving the monochromator, the beam of light oscillates between the reference and the sample portions of the instrument at a rate of 15 cycles per second. Constant reference energy with changing wavelength is maintained by an automatic servo system connected with the slit controlling the beam as it emerges from the monochromator. This system may be switched out of the circuit, however, if manual control of the beam is desired.

The monochromator is equipped with an automatic drive system which gives a linear variation of wavelength with time over five different time ranges. This, combined with a choice of paper speeds in the

recorder, provides for a very flexible operation, while the double beam ratio principle eliminates effects due to voltage fluctuations, spectral response, tube characteristics and atmospheric disturbances. A variable sensitivity range permits operation under a wide variety of signal to noise conditions.

Optical absorption measurements in the infrared region were made with the Perkin-Elmer Model 12C Infrared Spectrometer. This is a single beam instrument with a range of 2-15 microns using a rock salt prism.

The radiation source used in this spectrometer is a carborundum rod which is electrically heated to 1300°C by an input of 200 watts. At this temperature the bar radiates essentially as a black body in the wavelength region covered by the instrument. The beam of radiation is focused and directed by a series of mirrors having chrome-aluminum surfaces and is detected by means of a gold leaf thermocouple which has a very short response time (less than 0.05 sec.). The beam is chopped at approximately seven cycles per second, and the thermocouple output is passed through an amplifier tuned to this frequency. The output of the amplifier is fed to a continuous recorder. Since the instrument is of the single beam type, it is always necessary to make two separate runs in each study, one without the sample (for reference) and one with the sample.

This instrument is equipped with a wavelength drive for continuous determinations over various portions of the total spectrum. The reference intensity can be controlled within certain limits by a series of slits which can be mechanically connected to the wavelength drive. A

gain control is provided for attainment of optimum signal-noise patterns on the recorder.

Both of these instruments were primarily designed for use with liquid or gaseous samples. Therefore it was necessary to develop special mounts to adapt the instruments for work with crystals.

In the Beckman spectrophotometer, these mounts consisted of wooden blocks one centimeter square and three centimeters long-the same size as a standard Beckman rectangular cell. The blocks were tunneled through and fitted with front plates containing a 1/32 inch diameter hole (Figure 1). The crystal was taped to the front plate which was then fastened to the block. Such a procedure allowed beams of equal area to pass through the reference and sample channels regardless of the shape and size of the crystal being studied. Trouble in this system arose when refraction of the light beam by the crystal was such that the beam did not fall on the lead sulfide detector. The best solution found to this problem was a trial and error placement of the crystal in the mount until the beam did fall on a sensitive portion of the detector.

For the infrared work a plate was designed to fit the liquid absorption cell holder furnished with the instrument. This plate contained a 1/16 inch square hole in its center (Figure 2). A crystal could be taped over the hole exposing a standard shape and size to the instrument independent of crystal dimensions. A slight shift of certain standard absorption peaks observed during the sample cycle of the analysis was probably caused by the refraction of the beam while passing through the sample. No attempt to overcome this effect was

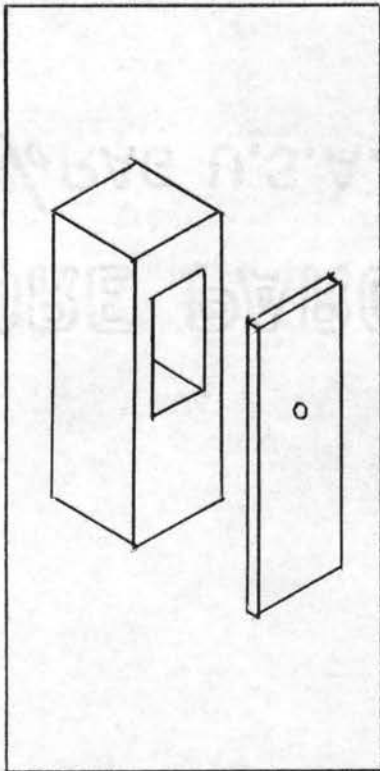


Figure 1. Mount for
Beckman Spectrophotometer

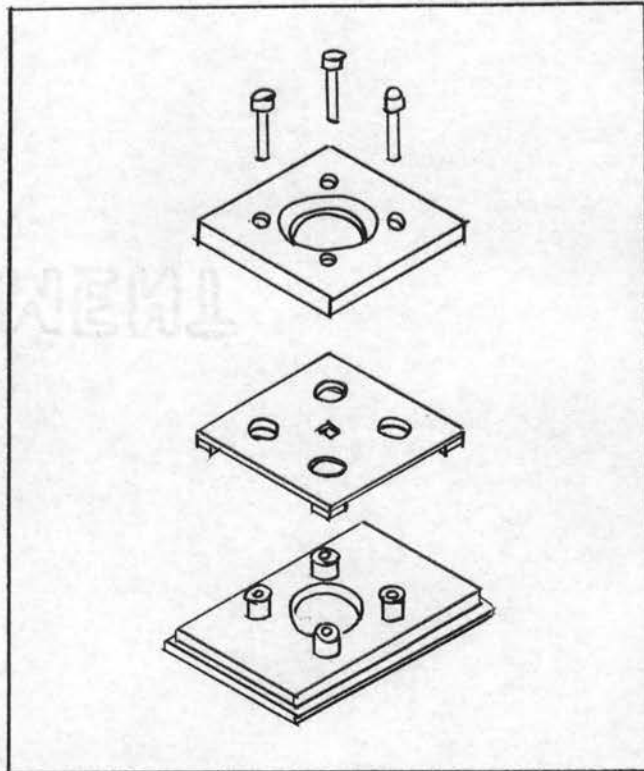


Figure 2. Mount for Perkin-Elmer
Spectrometer

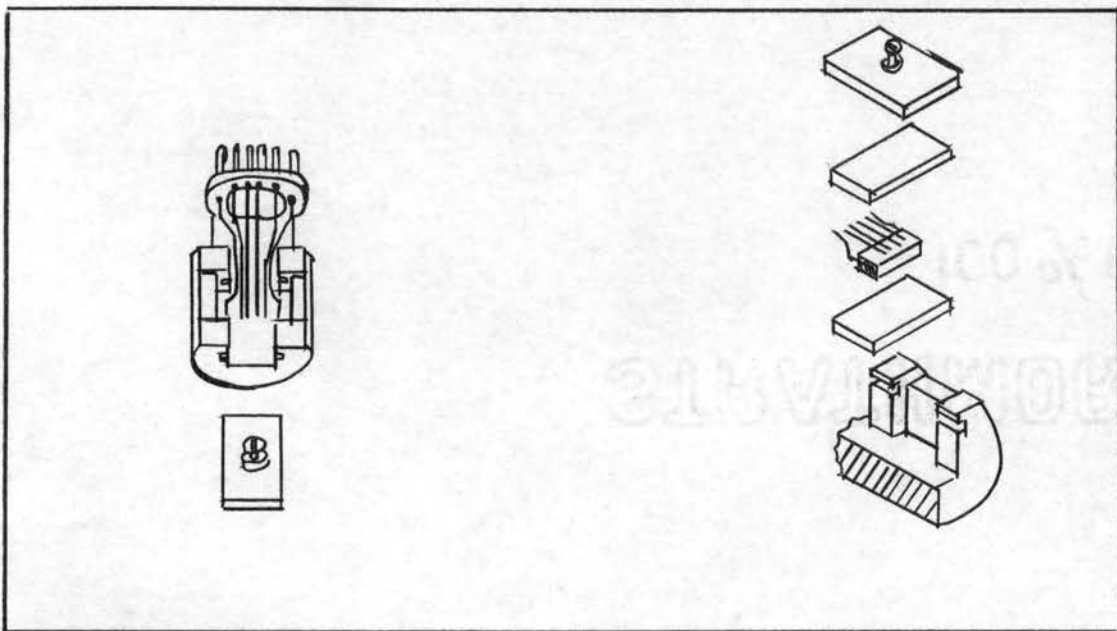


Figure 3. High Temperature
Conductivity Mount

Figure 3a. Cutaway view

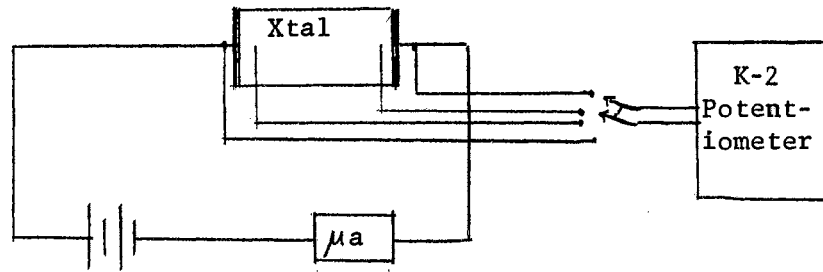


Figure 4. Circuit Schematic for Room Temperature Resistivity Measurements

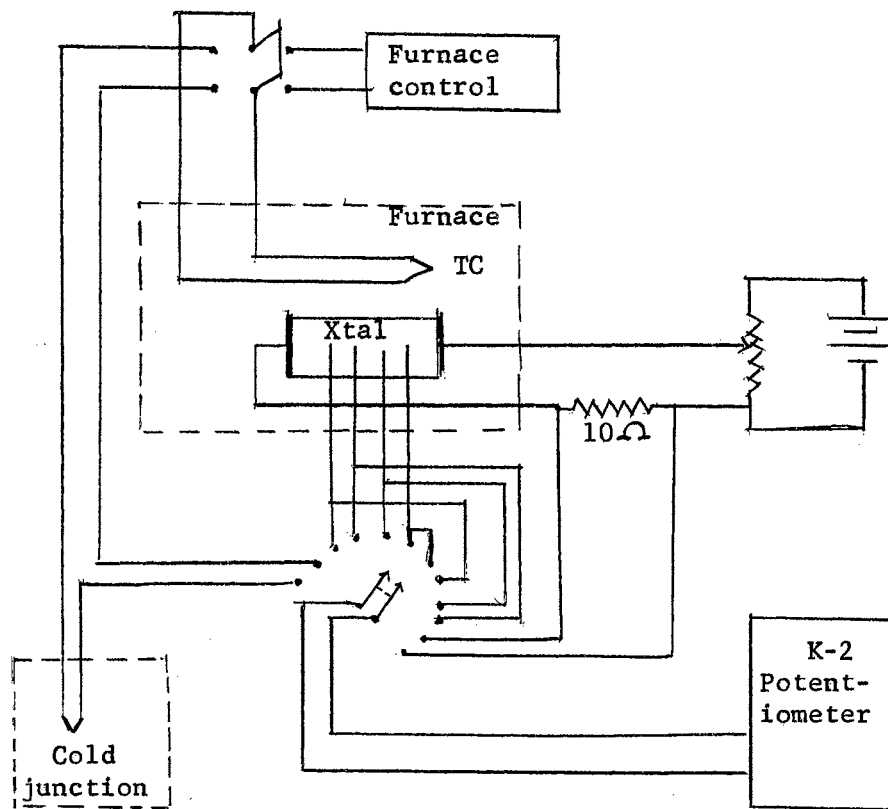


Figure 5. Circuit Schematic for Conductivity vs. Temperature Measurements

made in the instrument, although the deviation was taken into account in the calculation of percentage transmission.

D. Conductivity Equipment

Conductivity measurements at room temperature were made with an ordinary micromanipulator stage and a Leeds and Northrup Type K-2 Potentiometer. The circuit (Figure 4) was designed to allow measurement of the voltage drop across the contacts as well as across the sample itself.

Contacts were made to the ends of the crystal with the aid of silver paint (DuPont 4817). The probe contacts were copper points under pressure with no flux used. It was found that certain points on the crystal surface were more sensitive than others. From all appearances the point contacts were essentially non-rectifying while the painted contacts were definitely rectifying.

For measurement of conductivity at high temperatures, a special mount was designed to fit a tube furnace. It consisted of a copper block into which the crystal could be mounted with facilities for making two end connections to carry the current and four voltage probes for potentiometer measurements (Figure 3). Four probes were provided so that simultaneous measurements could be taken over different portions of the crystal to test homogeneity, and to furnish an additional check on the readings.

The circuit used for the high temperature measurements is shown in Figure 5 and a description of its component parts is given in the following paragraphs.

1. Sample mount

As stated above, the sample mount was a copper block designed to give mechanical support to the sample and its connections. The end contacts to the sample during high temperature measurements were made by platinum plates held to the crystal by a flux of indium metal. This metal has a high surface tension in the liquid state and provided good electrical contact between the crystal and the platinum above 150°C. Below this temperature the contact resistance goes up rapidly but conduction was sufficient to give consistent, noise free readings down to room temperature. At low temperatures the end contacts were made by using Aquadag as a flux rather than indium. Aquadag, a colloidal dispersion of graphite, makes very good electrical contacts but does not dry to a mechanically solid connection. For mechanical stability, therefore, it was found necessary to use a small amount of the silver paint around the edges of each end contact.

The voltage probes at the surface of the sample consisted of No. 36 platinum wires. These were laid parallel across the surface of the sample and pressure was applied between two quartz plates by means of an Inconel spring (Figure 3a). This pressure was enough to give probe contact across the entire width of the sample. However, it was found that sensitivity was greatly increased if the platinum wires were dipped in melted indium before being mounted for high temperature work. Likewise a small amount of Aquadag brushed along the wire increased the sensitivity at low temperatures. Using this method it was possible to obtain potentiometric readings to the nearest microvolt on most of the

samples in the temperature range 250-800°C with the sensitivity falling off somewhat for lower temperatures.

2. Potentiometer network

The necessary potentiometric readings were taken on a Leeds and Northrup Type K-2 Potentiometer used in conjunction with a Leeds and Northrup Model 2420B Box Galvanometer. The potentiometer was equipped with an eleven position selector switch which made it possible to take readings across several portions of the circuit with a minimum of effort. The potentiometer circuit was designed so that voltage measurements could be taken across the total portion of the crystal covered by the probes as well as each of the three small subportions. This allowed the checking of readings by comparing the sum of the voltages across the subintervals with the voltage across the entire interval. Comparing the resistivities of the subintervals gave a measure of the homogeneity of the crystal.

The current through the sample was measured by a potentiometric reading of the voltage drop across a standard ten ohm resistor placed in series with the current leads to the crystal. A Chromel-Alumel thermocouple embedded in the mount could also be switched into the potentiometric circuit so that the temperature of the sample could be determined in conjunction with each set of voltage and current readings. A normal cycle of readings at a given temperature consisted of: thermocouple voltage, probe voltages, voltage across the standard resistor, and a second thermocouple voltage measurement to detect any temperature drift.

3. Temperature control

The furnace used in these measurements is a Hoskins Tube Furnace, Model FH303. It is equipped with a current limiting rheostat for rough control of the furnace temperature between 550° and 1100°C . Actual control of the temperature for the experimental measurements was furnished by a Leeds and Northrup Speedomax Type G Recorder in conjunction with a Leeds and Northrup Series 60 Control Unit. It allowed the temperature of the sample to be brought to equilibrium at any value and maintained within two degrees of that value while the potentiometric readings were being taken. The thermocouple mounted in the sample block was used as the control thermocouple, being taken out of the circuit only while being read on the potentiometer.

4. Other components

The sample mount was placed in a Vycor tube which could be evacuated so that all measurements were taken under forepump vacuum conditions. The platinum leads from the sample were spot welded to No. 18 copper wire which was brought out of the tube through a hermetic seal in the end cap. Guides for the lead out wires consisted of small hermetic seals, with the voltage probes being brought out through one set of guides and the current leads and thermocouple wires being brought out separately. This system minimized the possibility of breakdown at high temperatures causing erroneous readings. Also the copper wires and their guides gave mechanical stability to the system while it was being moved, placed in the Vycor tubing, etc. The current in the crystal was controlled by a voltage divider in the current circuit

so that the maximum power dissipation in the crystal was kept below one milliwatt.

The low temperature measurements were taken by immersion of the Vycor tube in a dry ice-acetone bath. Dry ice was added to acetone until this solution was at a temperature near -50°C . The tube containing the sample was then placed in the bath and measurements were taken as the temperature of the bath rose to room temperature.

CHAPTER IV

OPTICAL DATA AND CALCULATIONS

The room temperature optical data taken in this study is presented in the form of percent transmission vs. wavelength. Because of the orientation with which the samples were cut, the data was taken with the beam of light incident in a direction parallel to the optic axis. The results for individual samples are given in the following paragraphs. Energy calculations are based on the assumption (50, 51) that absorption occurs only for those photons whose energy corresponds to an allowed transition from the valence band (or a donor level) to the conduction band (or an acceptor level). For use in quantitative calculations involving the short wavelength absorption edge, the wavelength at which the extended straight line portion of the transmission spectrum crosses the zero line has been arbitrarily chosen.

Table I presents a resume' of the important characteristics of the transmission spectra of each sample together with changes in these characteristics produced by heat treatment.

Sample I

At the beginning of the study this sample was chosen from the opaque portion of a natural cassiterite crystal so that the conductivities of opaque and clear portions of the crystal could be compared. Therefore no optical data could be obtained.

However, after the sample had been heated to 500°C for conductivity measurements, it was noticed that it had become more transparent at one end. Cracks that had developed made it useless for further conductivity work, so it was decided to see if oxidation would further change the optical properties. The sample was heated in air to 700°C and kept at that temperature for three hours. When it was removed from the furnace it was transparent and had a yellow-green color throughout the bulk with a dark red color near the edges. Further heating at 850°C for nine hours (again in air) caused the red coloration to move into all but a small interior portion of the crystal. After the final heating, transmission measurements were taken on both the green and the red portions (Figure 6).

For the green portion, the short wavelength cutoff was found at 430 millimicrons. The curve rose to a maximum near 800 millimicrons and then sloped off to a long wavelength cutoff near 2050 millimicrons. The break in the curve near 500 millimicrons is assumed to be the result of some red coloration of part of the surface.

The red portion showed a short wavelength cutoff near 550 millimicrons, a peak between 800 and 900 millimicrons, and a long wavelength cutoff near 2900 millimicrons.

Sample II

At the beginning of the study the clear portion of this sample gave a transmission spectrum having a short wavelength cutoff at 355 millimicrons and a long wavelength cutoff at 7.5 microns. Two small dips, possibly absorption peaks, were noted at 850 millimicrons and

1200 millimicrons, and one very definite and sharp absorption peak occurred at 3.75 microns (Figure 7). Unsuccessful attempts were made to take a transmission spectrum on the brown end.

After the sample had been used for conductivity measurements, during which it was heated to 800°C in vacuum, a transmission spectrum was again taken. The short wavelength cutoff was still at 355 millimicrons. The absorption noticed before at 850 millimicrons did not appear, but there was still evidence of absorption near 1200 millimicrons. Also there appeared to be a wide absorption region between 2 and 3 microns. Unfortunately, the surface of the crystal had been slightly eroded by the heat treatment so that a transmission spectrum in the infrared region could not be obtained.

Sample III

This sample gave a transmission spectrum having a short wavelength cutoff at 355 millimicrons and a long wavelength cutoff at 7.5 microns. There was a definite absorption peak at 3.75 microns but no indication of absorption at any other wavelength (Figure 8).

Sample SI

This sample, although very transparent, gave a different transmission spectrum from the other clear samples. The short wavelength cutoff was at 360 millimicrons (nearly the same as Samples II and III), but the long wavelength cutoff was at 1800 millimicrons (Figure 9). After the sample had been used for conductivity measurements (heated to 500°C in vacuum), the short wavelength cutoff remained the same but the long wavelength cutoff shifted to 2500 millimicrons.

Sample AI

The transmission spectrum of this sample indicates a short wavelength cutoff at 355 millimicrons and a long wavelength cutoff near 2900 millimicrons (Figure 10). There seems to be a wide absorption region extending from 800 to 1150 millimicrons.

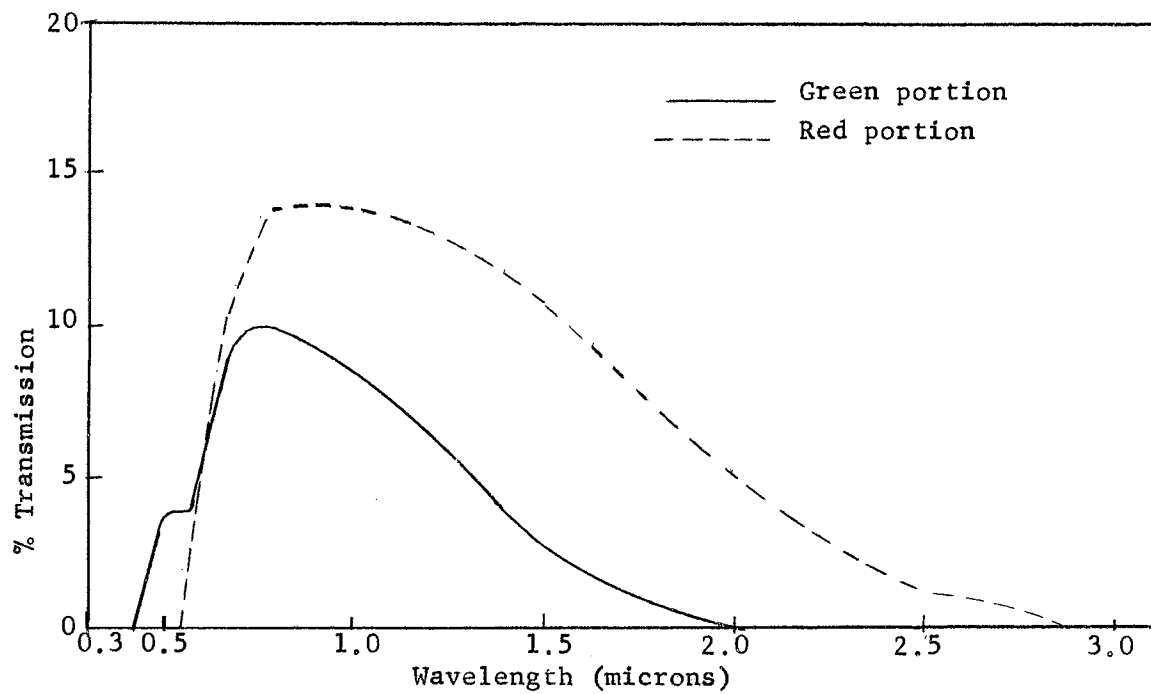


Figure 6. Transmission Spectrum of Sample I.

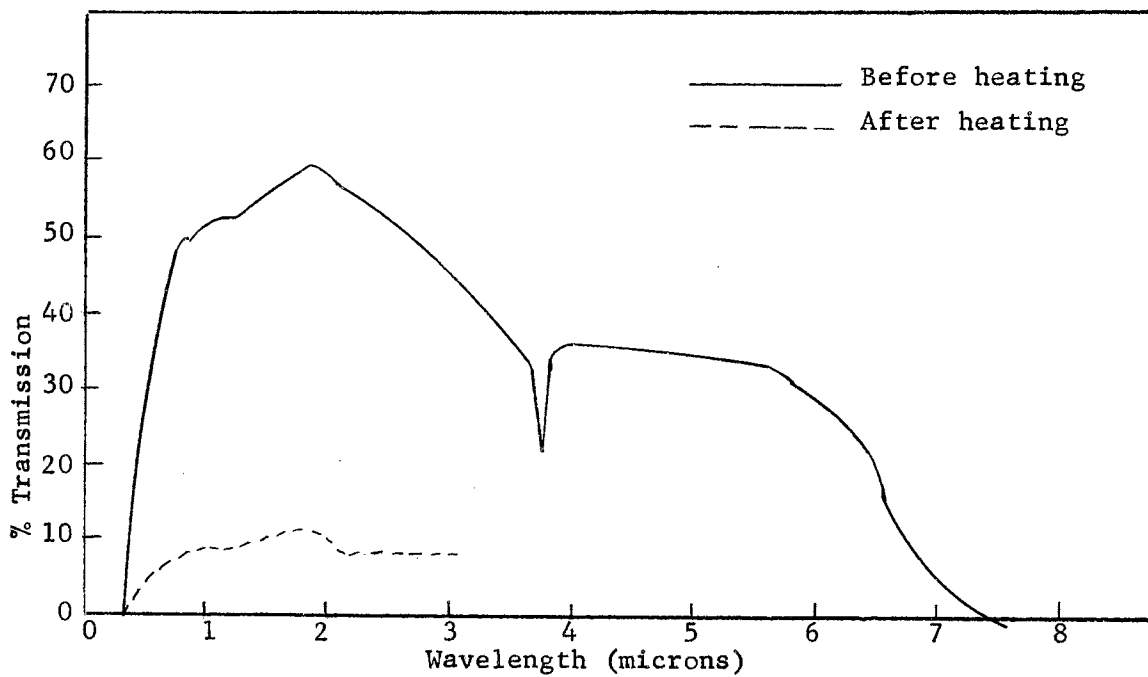


Figure 7. Transmission Spectrum of Sample II.

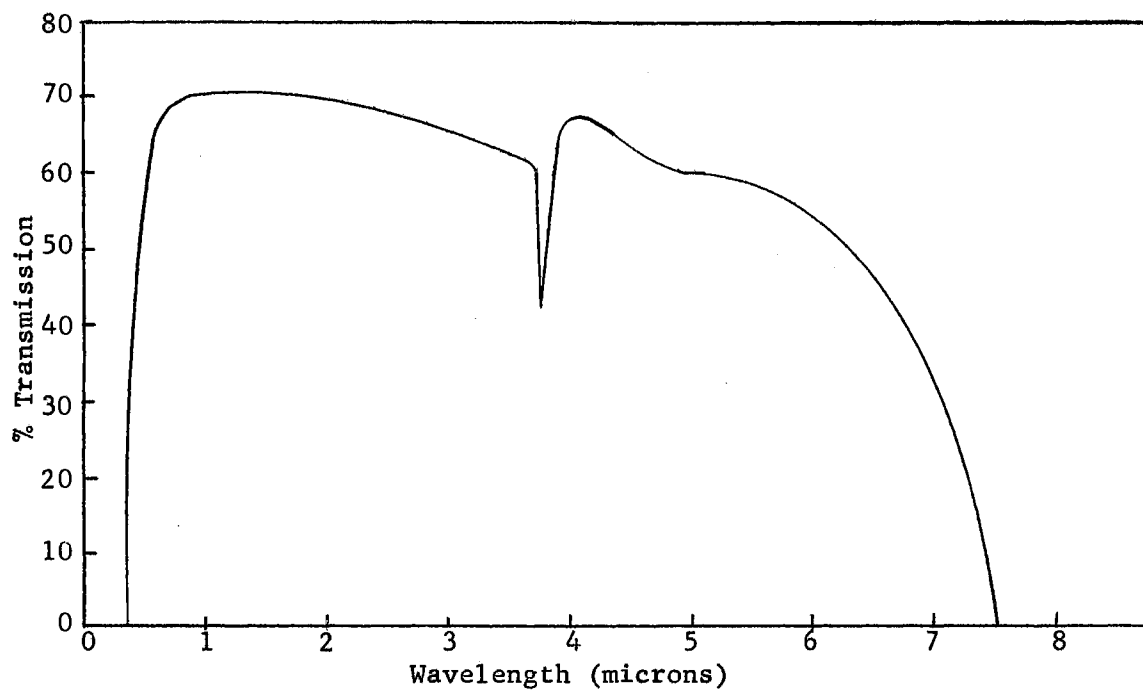


Figure 8. Transmission Spectrum of Sample III.

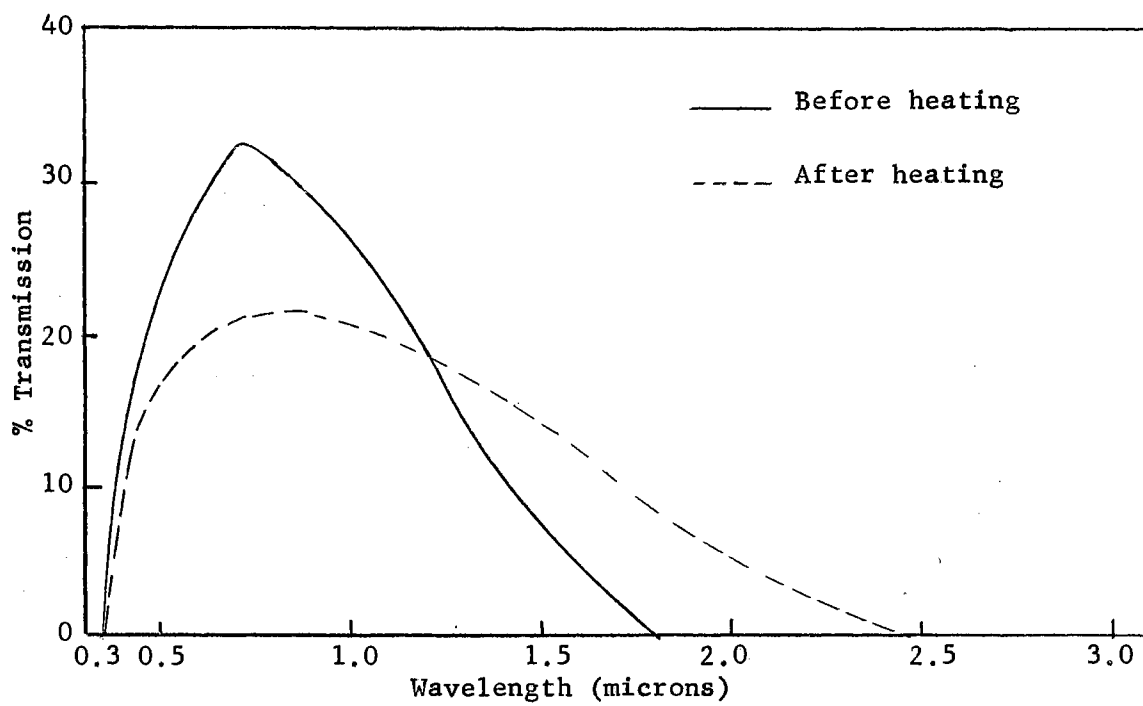


Figure 9. Transmission spectrum of Sample SI.

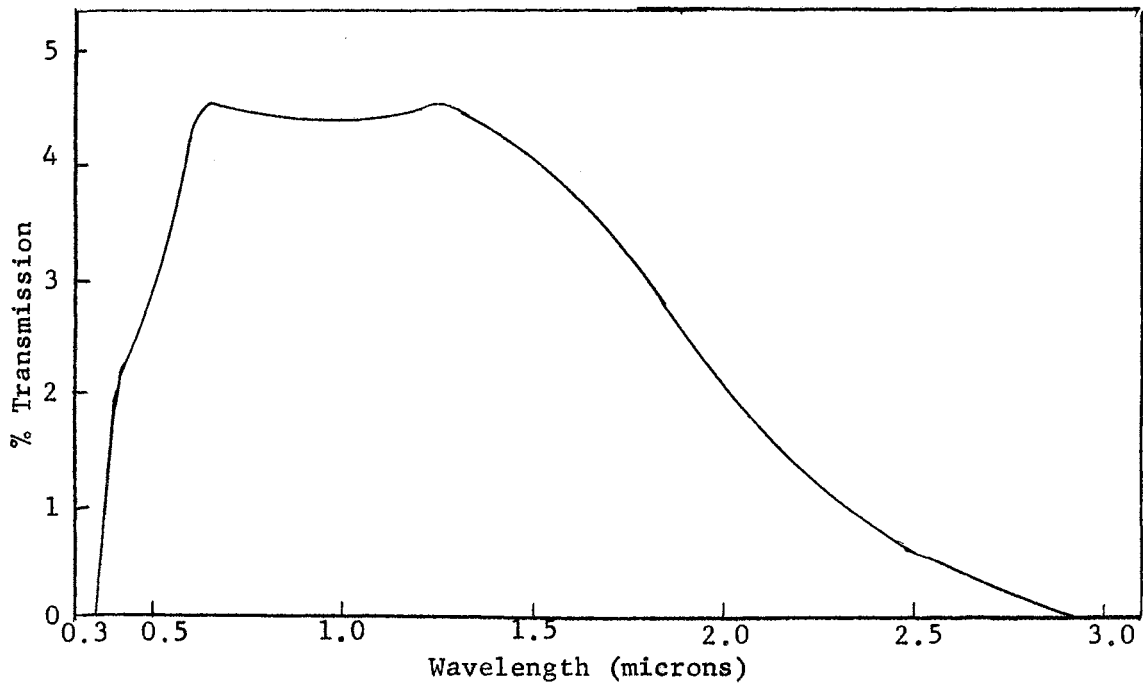


Figure 10. Transmission Spectrum of Sample AI.

TABLE I

TABULATED OPTICAL DATA AND CORRESPONDING ACTIVATION ENERGIES

<u>Characteristic</u>	<u>Sample</u>	<u>Wavelength</u> (microns)	<u>Energy</u> (ev)
Ultraviolet	I (green)	0.430	2.88
Absorption edge	I (red)	0.55	2.25
	II	0.355	3.49
	III	0.355	3.49
	SI	0.36	3.44
	AI	0.355	3.49
	Infrared cutoff	I (green)	2.05
I (red)		2.9	0.43
II		7.5	0.165
III		7.5	0.165
SI (before)		1.8	0.688
SI (after)		2.5	0.495
AI		2.9	0.43
Absorption regions		II (before)	0.85 (?)
		1.2 (?)	1.03
		3.75 (sharp)	0.33
	II (after)	0.85 missing	
		2-3	0.41-0.62
	AI	0.8-1.15	1.08-1.55

CHAPTER V

ELECTRICAL MEASUREMENTS AND CALCULATIONS

A. Preliminary measurements

Preliminary electrical measurements were taken on four of the samples to determine their approximate resistivity and to locate any sources of trouble that might arise in conductivity measurements. The orientation of the optical samples was such that all conductivity measurements were taken perpendicular to the optic axis. During the course of these measurements a cursory investigation was made of rectification by the end contacts and photoconducting phenomena were observed. The results of these exploratory studies are given in the following paragraphs.

1. Room temperature resistivity

The resistance across the major part of the crystal was measured and the resistivity calculated subject to the following assumptions:

(a) The equipotential surfaces were planes and were parallel to the ends of the crystal containing the current contacts.

(b) The conductivity was a bulk effect so the resistivity could be calculated by the equation,

$$\text{Resistivity} = \frac{\text{resistance} \times \text{cross-sectional area}}{\text{distance between probes}}$$

Results:

<u>Sample</u>	<u>Resistivity (ohm-cm.)</u>
I	2.4 to 4.2
II	2.4×10^4
III	1.8×10^4
SI	Very low ($\ll 1$)

2. Contact rectification

The resistance across the silver paint end contacts of Samples I and III was measured as a function of direction of current. Forward bias was found when the crystal was negative with respect to the metal. This n-type conduction is what would normally be expected of a reduction type semiconductor.

An example of the measured resistance of each end contact is given below under conditions of forward and reverse bias, together with the effective front to back resistance ratio.

<u>Sample</u>	<u>Resistance (ohms)</u>		<u>F/B ratio</u>
	(Forward)	(Reverse)	
I	1890	6380	3.4
	1990	3590	1.8
III	0.75×10^4	1.1×10^4	1.5
	2.16×10^5	8.86×10^5	4.1

3. Photoconductivity

Although no quantitative work was done on photoconductivity, certain observations were made concerning this effect. While the sample was mounted in the end contacts, total end-to-end resistance

under irradiation was measured with an ohmmeter, using both visible and ultraviolet light. The resistance rise was very slow and its relaxation time upon removal of the light appeared to be of the order of hours. An unsuccessful attempt was made to find photoconductivity peaks using an a-c method (52) indicating the necessity for modified techniques. No phosphorescence was observed even after intense ultraviolet irradiation.

The order of magnitude of the resistance change observed is given below:

<u>Sample</u>	<u>Resistance (ohms)</u>		
	<u>Dark</u>	<u>Visible light</u>	<u>Ultraviolet light</u>
II	8.7×10^5	8.2×10^5	4.0×10^5
III	8.0×10^4	6.5×10^4	1.5×10^4

B. Conductivity vs. Temperature Data

In calculating the conductivities of these samples, the same assumptions were made as were made in the room temperature resistivity measurements. Although there are indications that part of the conductivity is a surface phenomena, d-c measurements do not give a quantitative picture of how the total current is divided. For this reason, the magnitudes of the conductivities may be off by a constant factor for each sample. This, however, should not affect the slopes of the curves from which the activation energies were calculated. These activation energies (ΔE) have been calculated from various straight line portions of the curves using a Boltzmann relation of the form (53).

$$\sigma = \sigma_0 e^{-\frac{\Delta E}{kt}}$$

Since at the present stage of the work information concerning the values of the Fermi level is not available, the usual factor of two in the denominator implying intrinsic behavior at high temperatures and extrinsic behavior at low temperatures has been omitted in computing and tabulating results. The procedure and results for each sample are indicated below and the activation energies for certain temperatures are given in Table II.

Sample I

Measurements were taken on this sample between room temperature and 500°C (Figure 11). Evidence indicates that the crystal is inhomogeneous. Straight line portions of the conductivity curve appear in the regions $380\text{-}500^{\circ}\text{C}$ and $140\text{-}210^{\circ}\text{C}$.

Sample II

Measurements were taken on this crystal in the ranges $30\text{-}460^{\circ}\text{C}$, $350\text{-}780^{\circ}\text{C}$, and $(-40)\text{-}40^{\circ}\text{C}$. It showed some inhomogeneity in the magnitudes of the conductivity (Figure 12), but gave rather consistent results as to the slope of the conductivity vs. temperature curves in its subsections. The curves for the three measurements were matched in the overlapping regions to give one complete curve covering the temperature range $(-40)\text{-}800^{\circ}\text{C}$ (Figure 13). Straight line portions of this curve occur in the ranges $(-40)\text{-}40^{\circ}\text{C}$, $410\text{-}550^{\circ}\text{C}$, and $710\text{-}775^{\circ}\text{C}$.

Sample SI

Measurements on this sample were run in the temperature region $200^{\circ}\text{-}400^{\circ}\text{C}$. Contact problems prevented measurements at temperatures

lower than 200°C and the readings became unstable above 400°C . Whether the instability was a contact phenomenon or was caused by changes within the crystal itself is not known at this time. A straight line portion occurs in this curve in the temperature range $200\text{-}350^{\circ}\text{C}$.

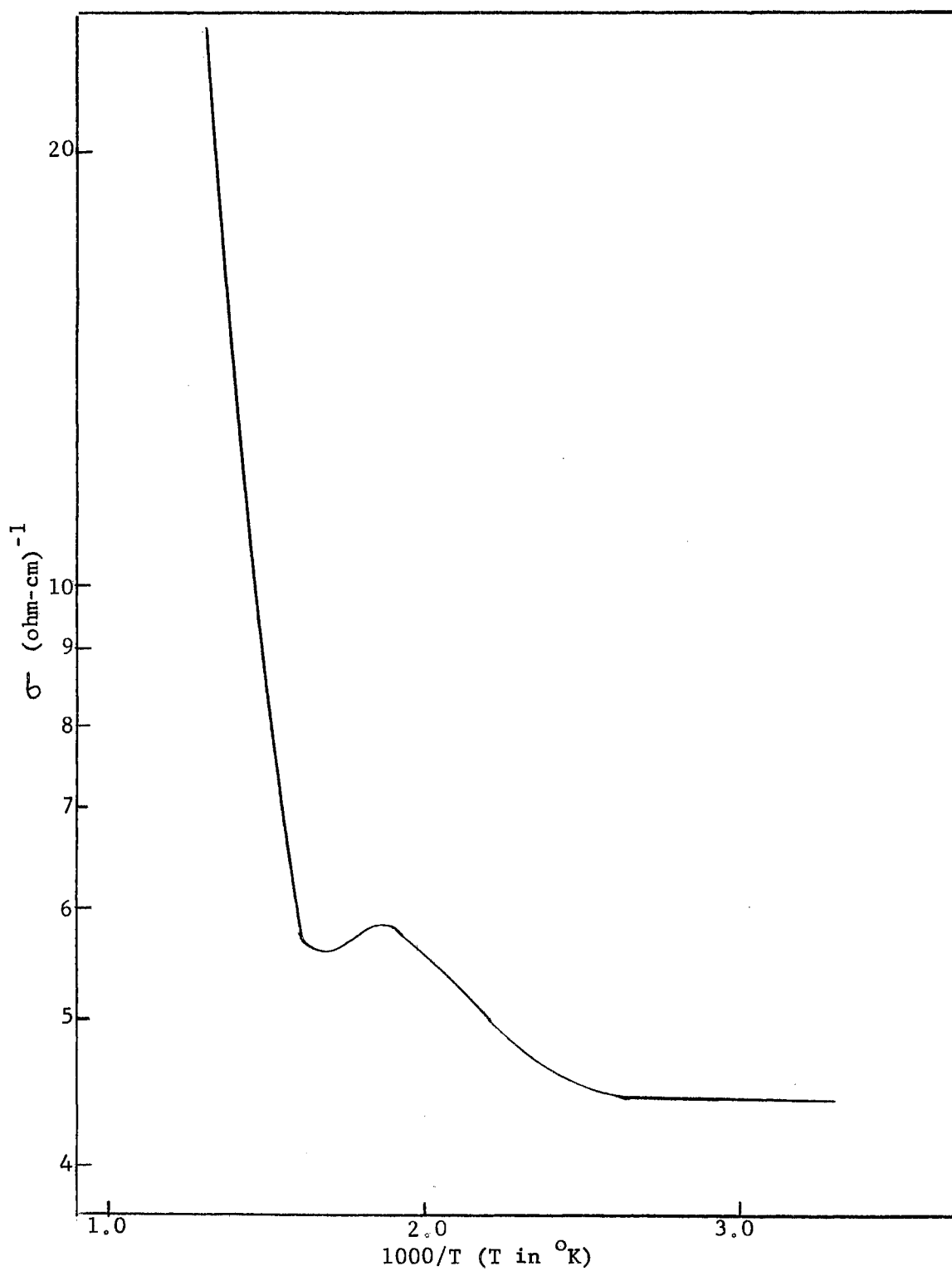


Figure 11. Conductivity vs. Temperature Curve for Sample I.

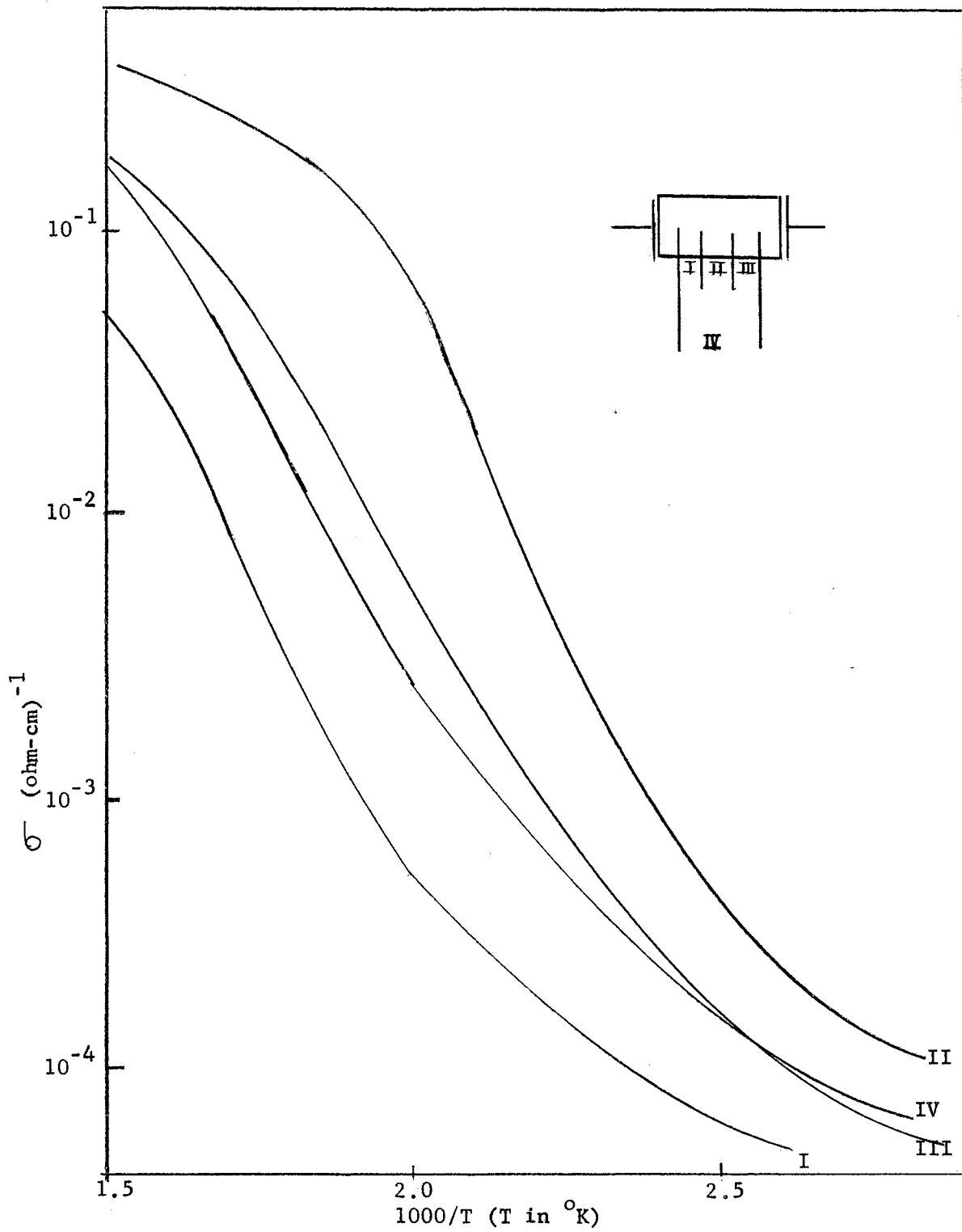


Figure 12. Conductivity vs. Temperature Curve Showing the Degree of Homogeneity in Sample II.

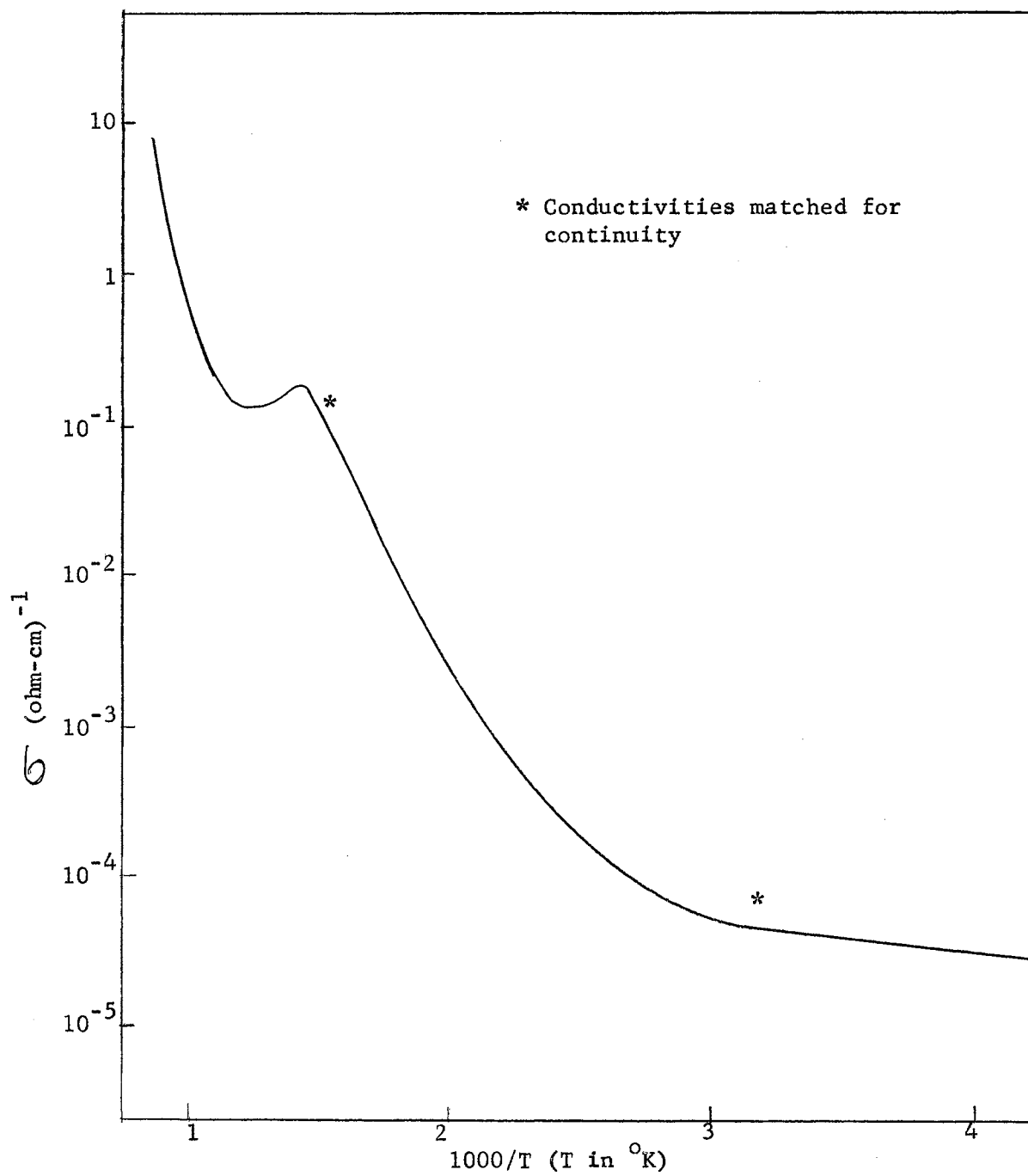


Figure 13. Conductivity vs. Temperature Curve for Sample II.

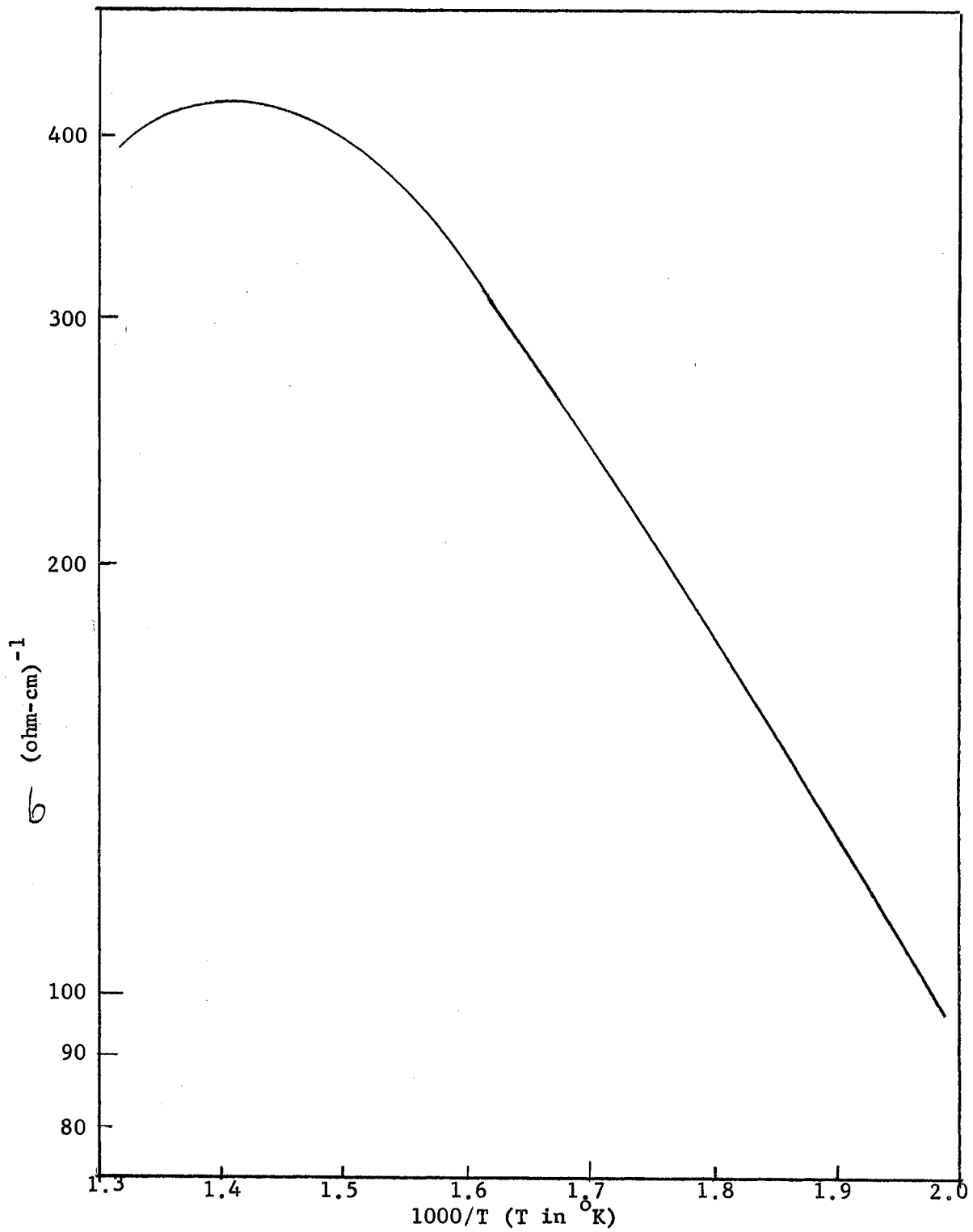


Figure 14. Conductivity vs. Temperature Curve for Sample SI.

TABLE II
CALCULATED ACTIVATION ENERGIES AND TEMPERATURE RANGES IN
WHICH THEY WERE FOUND

<u>Sample</u>	<u>Temperature range ($^{\circ}\text{C}$)</u>	<u>Activation energy (ev)</u>
I	140-210	0.04
	380-500	0.69
II	(-40)-40	0.035
	410-550	0.62
	710-775	1.12
SI	200-350	0.28

CHAPTER VI

CONCLUSIONS AND SUGGESTIONS FOR FURTHER STUDY

A. Correlation of Optical and Thermal Activation Energies

In working with a crystal having a large variation between its optical and static dielectric constants, a problem arises in the correlation of optical and thermal activation energies. By the Franck-Condon principle, more energy will be required to free an electron optically than thermally because of the difference in ion position during the processes. Mott and Gurney (50) show that the ratio of the optical activation energy to the thermal activation energy should be on the same order of magnitude as the ratio of the static dielectric constant to the optical dielectric constant. Breckenridge and Hosler (3) suggest that the ratio of activation energies in rutile is near five, although the ratio of dielectric constants is near twenty. Using similar considerations, it might be expected that the optical activation energy in cassiterite would be between two and five times the thermal activation energy. While the data obtained does not support any one ratio exclusively, some correlation appears to exist if it is assumed that the optical activation energy is equal to five times the thermal activation energy. Table III and the comments following give a list of possible activation energies corresponding to the data and certain considerations as to their significance. Reference to Tables I and II will show the evidence supporting each of the listed levels.

TABLE III
CORRELATED ACTIVATION ENERGIES

<u>Optical Activation Energies</u> (ev)	<u>Optical Activation Energies/5</u> (ev)	<u>Thermal Activation Energies</u> (ev)
		1.12
3.45	0.69	0.62-.69
2.88	0.58	
2.25	0.45	
1.50	0.30	0.30
1.05	0.20	
0.60-0.40	0.12-0.08	
0.33	0.067	
0.17	0.033	0.035-0.04

Comments:

(1) It is quite possible that the activation energy of 1.12 ev is low and that the slope of the conductivity vs. temperature plot is still increasing slightly for temperatures above the measured range. Foex (43), in his work on pressed powders, gives slopes corresponding to activation energies in the range 1.15 to 1.99 ev. However his findings also reflect a variation of this energy with the atmosphere surrounding the material, being higher for oxidizing atmospheres and lower for reducing atmospheres.

If the slopes observed in this region represent intrinsic transitions, the corresponding energies would be twice those reported here. The work of Breckenridge (3), however, seems to indicate that these are not intrinsic energies.

(2) Although activation energies are found in the region 0.2 to 0.4 ev, they show a large variation in different samples. Foex (43) reports two samples having an activation energy near 0.38 ev while this study has found energies near 0.2 ev in some samples and near 0.3 ev in others. These energies may be associated with foreign impurities, rather than oxygen vacancies or reduced tin atoms.

(3) The mechanisms producing the 0.08 to 0.12 ev reduced optical activation energies could be the ones responsible for the variation in the order of magnitude of the resistivities observed in the different samples. All of the low resistivity samples showed cutoff in this area, while the high resistivity samples did not. It is quite plausible that this cutoff is the result of an overlapping of wide absorption bands in the region 2-7 microns, due to a high concentration of impurity or vacancy centers.

B. Suggestions for Further Work

During the course of this work a number of problems have arisen which need to be studied in more detail. Also there are certain standard semiconductor studies which have not yet been attempted. In the list below, the first six items are suggested as immediate extensions of the present investigation and the rest are fields in which work needs to be initiated.

(1) Photoconductivity measurements for correlation with optical transmission data. It may be possible to resolve some of the broad absorption bands into peaks by means of photoconductivity measurements.

(2) Optical measurements at very low temperatures. These could prove very helpful in resolving optical bands into peaks, especially in the ultraviolet region and the two to seven micron band.

(3) A series of cyclic conductivity measurements while heating and cooling the sample. This would give a measure of the changes introduced in the sample as a result of the conductivity studies themselves. Work of this sort has been done on PbS by Scanlon (54) and shows definite changes within the samples during the measurements.

(4) Controlled oxidation and reduction of a sample with optical and/or conductivity measurements taken at various stages in the process. Determination of weight changes might give a measure of the variation in the number of oxygen vacancies which could then be correlated with the semiconductor studies. Such experiments would help to identify the activation energies associated with conductivity changes effected by these processes.

(5) Conductivity measurements as a function of frequency. These can give a measure of the relative importance of surface and bulk conductivities.

(6) Correlated spectroscopic studies on measured samples to determine the types and concentrations of impurities.

(7) Hall effect vs. temperature measurements for determining carrier concentrations and mobilities.

(8) Carrier lifetime measurements.

(9) X-ray diffraction studies to determine the concentration of interstitial ions and atoms.

(10) Study of the rectification curves at various types of contacts.

(11) Thermoluminescence measurements to determine position and depth of trapping levels.

These studies would provide a profitable addition to the understanding of the properties of cassiterite, even though they are limited by the experimental problems encountered in working with natural crystals. In addition, concurrent work leading to a procedure for the controlled growth of artificial cassiterite crystals should be carried on.

BIBLIOGRAPHY

1. Cronemeyer, D. C., and M. A. Gilleo, "The Optical Absorption and Photoconductivity of Rutile" Phys. Rev. 82, 975-976 (1951).
2. Cronemeyer, D. C. "Electrical and Optical Properties of Rutile Single Crystals." Phys. Rev. 87, 876-886 (1952).
3. Breckenridge, R. G., and W. R. Hosler. "Electrical Properties of TiO_2 Semiconductors." Phys. Rev. 91, 793-802 (1953).
4. Palache, C., H. Berman, and C. Frondel. "Cassiterite" Dana's System of Mineralogy. New York: John Wiley and Sons, Inc., 1944, pp. 574-581.
5. Weiser, H. B., The Hydrous Oxides. New York: McGraw-Hill, 1935, pp. 202-224.
6. Coffeen, W. W. "Ceramic and Dielectric Properties of the Stannates." J. Am. Ceram. Soc. 36, 207-214, (1953).
7. Quirk, J. and C. G. Harman. "Properties of a Tin Oxide-base Ceramic Body," J. Am. Ceram. Soc. 37, 24-26 (1954).
8. Berkman, S., J. C. Morrell, and G. Egloff. Catalysis. New York: Reinhold Publishing Corp., 1940.
9. U. S. Pat. 2,617,745 (Nov. 11, 1952) Pittsburgh Plate Glass Co.
10. Dutch Pat. 73,114 (August 15, 1953) N. V. Philips Gloeilampenfabriken.
11. U. S. Pat. 2,583,732 (Jan. 29, 1952) E. A. Ericsson and A. O. Jorgensen.
12. German Pat. 807,416 (June 28, 1951) E. Durrwachter.
13. Verwey, E. J. W. "Oxidic Semiconductors." Semiconducting Materials. Ed. H. K. Henisch. London: Butterworths Scientific Publications Ltd., 1951, pp. 151-161.
14. Gray, T. J. "On the Properties of Semi-conducting Oxides." Semiconducting Materials. Ed. H. K. Henisch. London: Butterworths Scientific Publications Ltd., 1951, pp. 180-187.
15. Gray, T. J. "Semiconductivity and Magnetochemistry of the Solid State." Chemistry of the Solid State. Ed. W. E. Garner. London: Butterworths Scientific Publications Ltd., 1955, pp. 133-142.

16. Thurnauer, H. "Review of Ceramic Materials for h-f Insulation." J. Am. Ceram. Soc. 20, 368-372 (1937).
17. Connell, L. F., and R. L. Seale. "Electrical Properties of Rutile Single Crystals." Phys. Rev. 85, 745 (1952).
18. Berberich, L. J., and M. E. Bell. "Dielectric Properties of the Rutile Form of TiO_2 ." J. Applied Physics 11, 681-692 (1940).
19. Johnson, G. H. "Influence of Impurities on Electrical Conductivity of Rutile." J. Am. Ceram. Soc. 36, 97-101 (1953).
20. Johnson, G., and W. A. Weyl. "Influence of Minor Additions on Color and Electrical Properties of Rutile." J. Am. Ceram. Soc. 32, 398-401 (1949).
21. Zerfoss, S., R. G. Stokes, and C. H. Moore. "The Properties of Synthetic Single Rutile Crystals." J. Chem. Phys. 16, 1166 (1948).
22. Weyl, W. A., and T. Forland. "Photochemistry of Rutile." Ind. Eng. Chem. 42, 257-263 (1950).
23. Harmon, G. G. and R. L. Raybold. "High-Frequency-Induced Electroluminescence in ZnS." Phys. Rev. 104, 1498 (1956).
24. Matossi, F. "The Vibration Spectrum of Rutile." J. Chem. Phys. 19, 1543-1546 (1951).
25. Mitchell, E. W. J. "Impurity Scattering in Oxide Semiconductors" Proc. Phys. Soc. (London) 65B, 154-161 (1952).
26. Arzruni, A. "Kunstlicher Kassiterit." Zeitschrift fur Krystallographie XXV, 467-470. (1895).
27. Levy, M. and L. Bourgeois. "Sur le Dimorphisme de l'acide Stannique." Compt. Rend. Acad. Sci. (Paris) 94, 1365-1366 (1882).
28. Wunder, G. "Uber den Isotrimorphismus des Zinnoxyds und der Titan Saure und uber die Krystallformen der Zirconerde" J. Prakt. Chem. Ser. 2, Vol. 2, 206-212 (1870).
29. Bragg, W. L. "The Oxides." Atomic Structure of Minerals. Ithaca: Cornell University Press (1937) pp. 83-113.
30. Egli, P. H. (Private communication), Sept. 6, 1956.
31. Vegard, L. "Results of Crystal Analysis." Phil. Mag. (7) 1, 1151-1193 (1926).
32. Bollnow, O. F. "The Lattice Theory of the Crystals of TiO_2 , Rutile and Anatase." Z. Physik 33, 741-760 (1925).

33. Bragg, W. L., and J. A. Darbyshire. "The Structure of Thin Films of Certain Metallic Oxides." Trans. Faraday Soc. 28, 522-529 (1932).
34. Neuhaus, A., and W. Noll. "Crystal Chemistry of Cassiterite." Die Naturwissenschaften, 36, 26-27 (1949).
35. Himmel, H. "Optical Measurements on Cassiterite." Neues Jahrb. Mineral. Geol., Beil. Bd. A64, 67-70 (1931).
36. Gotman, J. D. "Some Anomalies in the Properties of Cassiterite." Compt. Rend. Acad. Sci. URSS 23, 470-472 (1939).
37. Ecklebe, F. "Optical Studies on Cassiterite in the Temperature Region 16-1100°" Neues Jahrb. Mineral. Geol., Beil. Bd. 66A, 47-88 (1933).
38. Berton, A. "Comparison of Visible and Ultraviolet Color of Mineral Oxides and their Hydroxides and Hydrates." Compt. rend. 207, 625-627 (1938).
39. Liebisch, T. "The Layer Structure and Electrical Properties of Cassiterite." Sitzb. kgl. Preuss. Akad. Wiss. 1911, 414-422 (1911).
40. Tonneson, T. H. "The Distribution of Transistor Action." Proc. Phys. Soc. (London) 65B, 737-739 (1952).
41. LeBlanc, M., and H. Sachse. "The Electron Conductivity of Solid Oxides with Different Valencies." Physik Z. 32, 887-889 (1931)
42. Guillery, P. "Electrical and Optical Behavior of Semiconductors. VI. Conductivity Measurements on Powders." Ann. Physik 14, 216-220 (1932).
43. Foex, M. "Study of the Electrical Conductivity of the Oxides of Ti, Sn and Ce as a Function of Temperature and of the Medium." Bull. Soc. Chem. France 11, 6-17 (1944).
44. Luckiesh, M. "Spectral Reflectances of Common Materials in the Ultraviolet Region." J. Opt. Soc. Am. 19, 1-6 (1929).
45. Bauer, G. "Electrical and Optical Behavior of Semiconductors. XIII. Measurements on Oxides of Cd, Tl, and Sn." Ann. Physik 30, 433-445 (1937).
46. Lyon, D. N., and T. H. Geballe. "The Temperature Coefficient of Resistance of Tin Oxide Coated Electrically Conducting Glass Between 1° and 300° K." Rev. Sci. Instrum. 21, 769-770 (1950).
47. Fischer, A. "Thin Semiconducting Layers on Glass." Z. Naturforsch. 9a, 508-511 (1954).

48. Aitchison, R. E. "Transparent Semiconducting Oxide Films." Australian J. Appl. Sci. 5, 10-17 (1954).
49. Andrievskii, A. T., and V. A. Zhuravlev "Relaxation of Photoconductivity of SnO_2 ." Dokl. Akad. Nauk. SSSR 108, 1, 43-46 (1956).
50. Mott, N. F. and R. W. Gurney. Electronic Processes in Ionic Crystals. Oxford: Clarendon Press, 1948, pp. 160-162.
51. Seitz, F. The Modern Theory of Solids. New York: McGraw-Hill Book Co., Inc., 1940.
52. Johnson, C. C. Master's Thesis, Oklahoma State University, 1958 (unpublished).
53. Shockley, W. Electrons and Holes in Semiconductors. New York: D. Van Nostrand Co., Inc., 1950.
54. Scanlon, W. W. "Interpretation of Hall Effect and Resistivity Data in PbS and Similar Binary Compound Semiconductors." Phys. Rev. 92, 1573 (1953).

VITA

John Willard Northrip II
Candidate for the Degree of
Master of Science

Thesis: OPTICAL ABSORPTION AND ELECTRICAL CONDUCTIVITY IN CASSITERITE

Major Field: Physics

Biographical:

Personal Data: Born in Tulsa, Oklahoma, July 7, 1934, the son of J. Willard and Vivian Northrip.

Education: Attended grade school in Tulsa, Oklahoma; graduated from West Plains High School, West Plains, Missouri in 1951; received a Bachelor of Science degree from Southwest Missouri State College in August, 1954; completed requirements for the Master of Science degree in May, 1958.

Experience: Entered the United States Navy in August, 1954, for a two year tour of duty. Attended Class A Electronics Technician School and served as a technician on radar and communications equipment.

Organizations: Member of Sigma Pi Sigma and Kappa Mu Epsilon.